Random telegraph signal and spin characteristics of the gate-all-around poly-silicon nanowire

Tsung-Han Lee, Yan-Ting Li, and Shu-Fen Hu

Random telegraph signal and spin characteristics of the gate-all-around poly-silicon nanowire

Tsung-Han Lee, Yan-Ting Li, and Shu-Fen Hu[a)]
Department of Physics, National Taiwan Normal University, Taipei 116, Taiwan

An arsenic (As)-doped poly-silicon nanowire gate-all-around transistor fabricated using standard semiconductor methods was used to measure the Coulomb blockade effect by applying a tunable gate voltage. Two-level trapping states due to the random telegraph signal of fluctuating drain current were observed in the silicon transport channel. Under high magnetic fields, the superposition points of differential conductance revealed weak 2-electron singlet-triplet splitting states of the arsenic magnetic impurity. The weak spin-orbital coupling suggests that the electron-spin-polarization in the As-doped silicon nanowire and the two-level trapping state coexisted in the Coulomb blockade oscillations. These characteristics indicate that a few arsenic donors strongly affect the quantum behavior of the poly-silicon material. © *2014 AIP Publishing LLC*.
[http://dx.doi.org/10.1063/1.4901196]

I. INTRODUCTION

Well-controlled, highly efficient standard semiconductor processes can be used to easily fabricate various nanoscale devices. With application of this technology to the manufacture of various solid-state quantum devices, the nanoelectronics of mesoscopic systems can be studied. The one-dimensional nanodevice is one such device; a quantum dot in a silicon nanowire is detected by Zeeman splitting of a single hole and is determined to be a ground-state spin configuration for one to four holes occupying the quantum dot.[1] Furthermore, a silicon nanowire with a surrounding gate, known as a gate-all-around (GAA) silicon nanowire,[2] can be fabricated using deep-UV lithography and oxidization.[3] A GAA PMOS silicon nanowire demonstrates the charge-trapping properties for mesoscopic system, the capture and emission time of random telegraph signal (RTS) noise is temperature dependent.[4] A related structure, the GAA twin silicon nanowire transistor, presents RTS with Coulomb blockade characteristics at room temperature.[5] In addition to the GAA structures of the nanowire, donor doped, such as arsenic, phosphorus, and boron, are essential in the transport channel of a silicon nanowire. For example, detecting resonant spin-up and spin-down electrons under a magnetic field can reveal two possible charge states occupied by the arsenic donors.[6] By using a temperature-dependent pumped current, the ionization energy of tunable multiple donors can be estimated.[7] Another important feature of a single arsenic donor in a silicon FinFET is the capability of controlling the degree of hybridization of a single electron donor state between the nuclear potential of its donor atom and a nearby quantum well.[8] By tuning the electrostatic coupling, series electrical transport can be observed through the doped and single-electron transistor.[9] In particular, by association, the one-electron (D^0) and two-electron (D^-) charge states of the arsenic donor consist of a pair of characteristic transport resonances. The atomic orbital of a single arsenic doped incorporated in a silicon nanostructure is tunable by the gate electric field, which is observed as an exotic transport resonance of the valley Kondo effect.[10]

In this study, we fabricated a GAA silicon nanowire field-effect transistor (FET) to investigate the effect of arsenic on the transport channel. By tuning, the gate voltage affects the trap states, which allows observation of the coupling of the electrons transport. Subjecting the source-drain bias to a high magnetic field induces the spin characteristic of the one-electron and two-electron charge states of the arsenic donor.

II. EXPERIMENTAL DETAILS

The devices were fabricated on n-type dummy wafers, which were first oxidized to form a buried oxide with a thickness of 200 nm. Amorphous silicon with a thickness of 200 nm was deposited on this substrate. Subsequently, negative photoresist of thickness 380 nm was coated on the wafer surface. The nanowire connecting the source and drain square-contact-blocks was patterned by electron-beam lithography. The reactive ion etching (RIE) process was used on the amorphous silicon to form the nanowire structure of the line with width of approximately 150 nm. Thereafter, a nitride hard mask with a thickness of 30 nm was applied to protect the amorphous silicon. The nitride hard mask of the E-beam lithography definition was removed by dry etching. Consequently, the nanowire area was exposed. The substrate was dipped in a buffered hydrofluoric acid solution to remove the buried oxide and to allow the nanowire to float, as shown in Fig. 1(a). Subsequently, dry oxidation treatment was applied to deplete the surface silicon, which facilitated the application of pattern-dependent oxidation (PADOX) to reduce the dimensions of the nanowire and to encircle the nanowire with SiO_2.[11,12] Poly-silicon with a thickness of 150 nm was applied as gate material to fill the surface of the substrate around the floating nanowire. A schematic of the poly-Si nanowire and surrounding gate is shown in Fig. 1(b). Through E-beam lithography patterning and RIE etching on the substrate, the silicon gate was formed. The arsenic was

a)Electronic addresses: sfhu.hu@ntnu.edu.tw and sfhu.hu@gmail.com
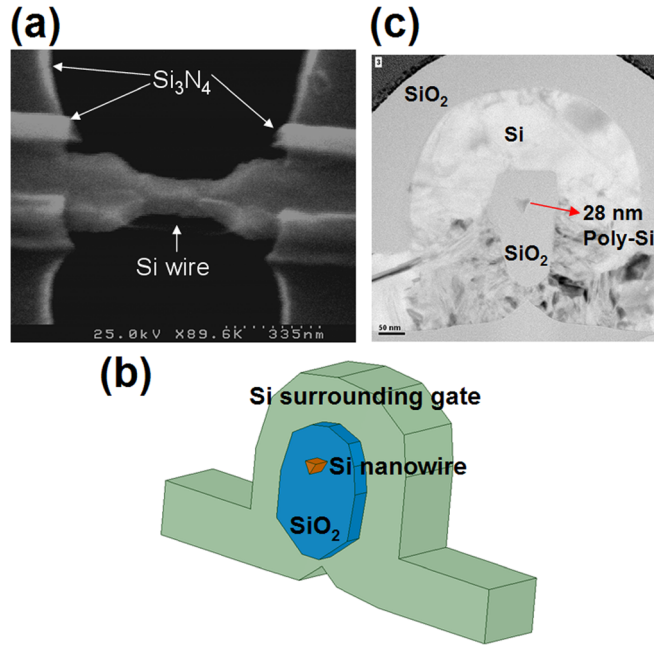
(a)

(c)

(b)

FIG. 1. (a) Oblique-view SEM image of the suspended silicon nanowire. (b) Schematic of the poly-Si nanowire and surrounding gate. (c) TEM image of the cross-section for the GAA nanowire device used to determine the dimensions of the nanowire.

deposited on the substrate and then the substrate was treated by rapid thermal annealing. 200 nm thick tetraethoxysilane was applied on the substrate. The electrode-contact holes were etched by E-beam lithography processing and RIE etching. Al–Si–Cu alloy with a thickness of 500 nm, which served as the electrode material, was deposited on the substrate and sintered at 400 °C in ambient nitrogen for 30 min. The cross section of the finished device, obtained through TEM, is shown in Fig. 1(c).

All measurements were performed at low temperature under high-magnetic fields. The nanowire device was bonded to a chip carrier and mounted on a sample holder. Using an Oxford variable temperature insert to measure the device properties, the magnetic and electric fields were measured at approximately 1.47 K. The electrical measurements of the nanowire device were configured using the four-terminal method with a Keithley 2602 dual channel source-meter.

III. RESULTS AND DISCUSSION

Figure 2(a) shows the contour plots of drain current I_D versus gate voltage V_G of the nanowire. I_D oscillation shows the Coulomb blockade diamond, which reveals the properties of the quantum dots in the device. The transport channel of the silicon nanowire was heavily implanted with arsenic; thus, a single atom impurity formed a quantum dot in the silicon channel of the nanodevice. This case is similar to the quantum dots of arsenic doped in a silicon nanowire systems.[1,6,9] The Coulomb diamond was used to determine the gate capacitance C_G and the tunnel-junction capacitances for the drain and source, C_D and C_S, respectively. The slopes of the sides of the Coulomb diamond are $C_D/C_G = 3.11$ and $-C_S/C_G = -4.27$. According to the difference of source-drain bias (ΔV_{DS}), C_Σ can be calculated
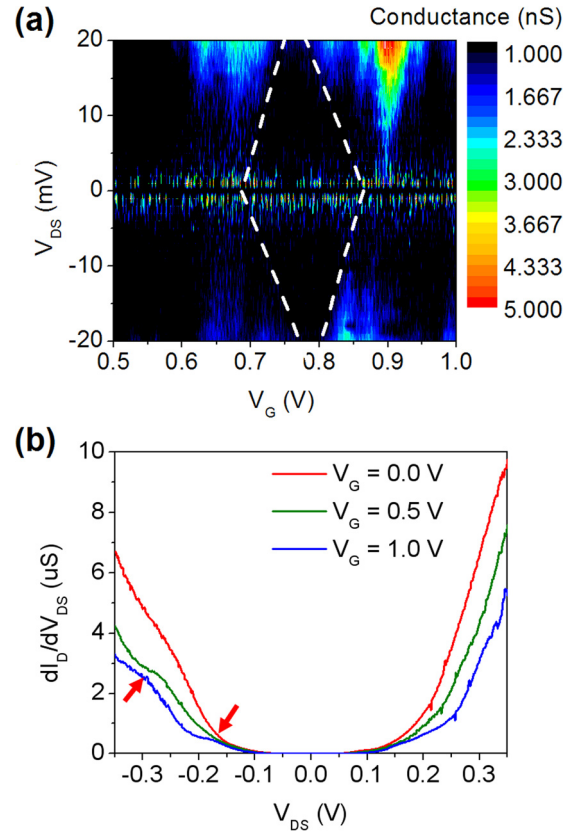
(a)

(b)

FIG. 2. (a) Contour plots show the visible conductance oscillation surrounding a Coulomb diamond. (b) The differential conductance (dI_D/dV_{DS}) as a function of V_{DS} for $V_G = 0$, -0.5, and -1.0 V.

as $C_\Sigma = e/\Delta V_{DS} = 6.65$ aF. Therefore, using the equation for total capacitance $C_\Sigma = C_S + C_D + C_G = 6.65$ aF, the capacitances C_S, C_D, and C_G can be determined as approximately 3.39, 2.47, and 0.79 aF, respectively.[13] The energy charge on the doped site is the fraction $\alpha = C_G/(C_S + C_D + C_G) = 0.119$ of V_G spacing. The charging energy was estimated as $Ec = e^2/C_\Sigma = 24.1$ meV.[6] The nanowire structure was assumed to have a concentric sphere total capacitance of $C_\Sigma = 4\varepsilon_r\varepsilon_0\pi R_1 R_2/(R_1 - R_2)$, where R_1 and R_2 are the diameters of the silicon nanowire and gate oxide, respectively; ε_0 is the dielectric constant of vacuum; and ε_r is the relative dielectric constant of SiO$_2$. Using $C_\Sigma = 6.65$ aF, the equivalent radius of the quantum dot was estimated to be 13.3 nm, which is consistent with the dimensions for half of the diameter of the silicon nanowire [28 nm in Fig. 1(b)]. According to the dose of the arsenic implantation is 5×10^{15} cm^{-2}, we can estimated the 2.67 arsenic ions in the quantum dots. This result suggests the quantum dots are due to arsenic donors in the silicon nanowire.

In addition, the differential conductance (dI_D/dV_{DS}) as a function of the source–drain bias (V_{DS}) for $V_G = 0$, -0.5, and -1.0 V, as shown in Fig. 2(b), gradually exhibited plateau characteristics. This is also a characteristic of the Coulomb blockade behavior.

The change in the two-level switching signals of I_D with increasing V_G is shown in Fig. 3(a). The histogram of the collected current data points, shown in Fig. 3(b), suggests two regions. The two distribution groups indicate that a two-level trap state coexists with the Coulomb oscillations.
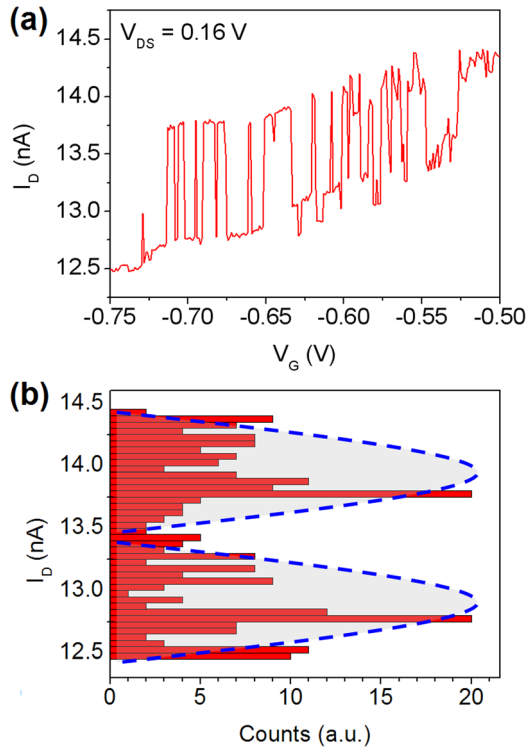
FIG. 3. (a) Transfer characteristics that exhibit two-level switching. (b) Counts of the two traces of (a) in a histogram.

FIG. 4. (a) Fluctuation of I_D due to tuning V_G, which controls capturing and emitting events, leading to the appearance of RTS in the nanowire device. (b) RTS changes in I_D versus source–drain bias showing linear fitting for $V_G = -0.65$ V; the obtained cut-off voltage is 89 mV. (c) Schematic of the model for the quantum dots and the trap position in the nanowire channel; QD is the quantum dot of the As donor, CB and VB are the conduction band and valence band.

The change in the drain current (I_D) with V_G for various V_{DS} from 0.11 to 0.20 V at 1.47 K is shown in Fig. 4(a). The discrete switching current signals reveal that the trapping state is a two-level RTS. The fluctuation of I_D with tunable V_G to control carrier capturing and releasing events caused RTS in the nanowire device. The I_D measurements exhibited RTS for V_G from -0.9 V to -0.4 V. The energy level of the trap state is fixed with respect to the conduction band edge. For this reason, the capturing or releasing characteristics only depend on the position of the trap level relative to the Fermi level.[14] Assuming that the electron capture is performed by an initially positive trap site (defect), then the lower current level corresponds to the trap-empty state (neutral), and the higher current level corresponds to the trap-filled state (negatively charged). The rapid switching of I_D increases the gate threshold voltage of the nanowire to randomly capture or release electrons until the trap-states are filled. Thus, the bias-dependent amplitude of RTS confirmed that the two-level trap state coexisted with Coulomb oscillations in the silicon nanowire.

The change in I_D due to RTS versus V_{DS} is linear for $V_G = -0.65$ V, as shown in Fig. 4(b). Unlike previous reports, the capture and emission containing either one or two electrons by a point defect are observed as the RTS in a silicon n-MOSFETs.[15] The nanowire device exhibits RTS characteristics that are a function of V_{DS}. A linear fit of the data in Fig. 4(b) gives a cut-off voltage of 89 mV, which can be used to estimate the energy difference between the Fermi level and the trap level. The assumed model for the trap position in the quantum dots in the nanowire channel is shown in Fig. 4(c). When $V_{DS} < 89$ mV, the Fermi level is below the trap level, implying that electrons must travel only through
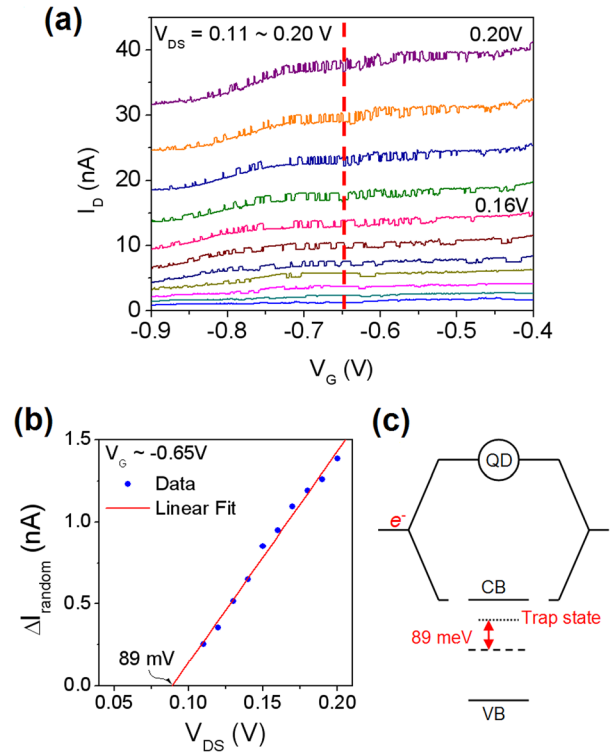
the quantum dot and not via the trap level. When $V_{DS} > 89$ mV, the Fermi level is higher than the trap level, hence the electrons from the source can move through both the traps and the quantum dots into the drain. Thus, a time-dependent RTS characteristic is superimposed onto the I_D of Coulomb oscillations. In addition, V_G can raise or drop the trap level relative to the Fermi level (V_{DS} fixing). By applying a particular V_G, the Fermi level deviates from the trap level, which the electrons were blocked into or filled up the trap states, thus time-dependent RTS disappears. For example, at $V_{DS} = 0.20$ [Fig. 4(a)], fluctuations in I_D are greatest at approximately -6.5 V, and the amplitude of the RTS characteristic gradually decreases above or below this value. This result suggests that V_{DS} can determine the threshold and amplitude of RTS; and V_G, through an electric field, can control the energy difference between the trap level and the Fermi level to tune the electron trapping ratio.

Unlike a non-equilibrium process in quantum dot, an electron tunnels into this dot, the telegraphic conductance of the RTS through the quantum point contact (QPC) is induced due to the electrostatic coupling between the quantum dot and QPC.[16] In our model, the time trace of RTS current is random and independent of the quantum dot. Thus, we have not shown the noise spectra as a function of the time trace.

Figure 5(a) shows the differential conductance (dI_D/dV_{DS}) as a function of magnetic field, where V_{DS} ranges from 0 V to 0.13 V. The $V_G = -1$ V figure shows distinct changes
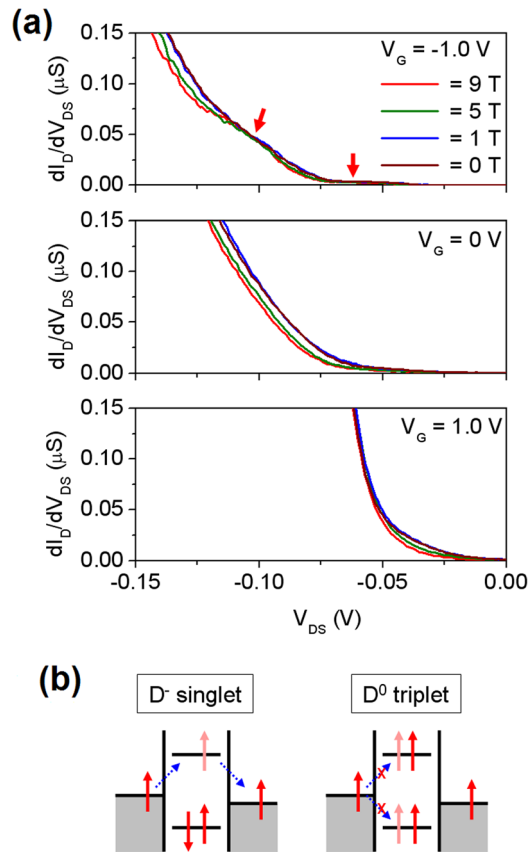
(a)

(b)

FIG. 5. (a) The dI_D/dV_{DS} is suppressed with increasing magnetic fields, as presented in the subfigures for $V_G = -1.0$, 0, and -1.0 V. At $V_G = 1.0$ V, two regions of the dI_D/dV_{DS} curves for varying magnetic fields overlap (red arrow marks), which suggests a singlet state of the donor. (b) The donor state is negatively charged (D$^-$), and the low-energy state is filled. The high-energy state can be filled by any spin electrons without being scattered by the magnetic field. When two spin-up electrons (D^0) occupy the low and high energy levels, the spin-up electrons will be scattered by the same spin electron of the orbital donor levels.

in slope of dI_D/dV_{DS} for various magnetic fields, but for $V_G = 0$ and 1 V, the slopes just rapidly increases. dI_D/dV_{DS} is suppressed weakly with increasing magnetic field, which suggests scattering of electrons by the magnetic field. Particularly, the two regions of dI_D/dV_{DS} (marked with red arrows and as "singlet") show overlapping multiple curves for varying magnetic fields, as shown for the $V_G = -1$ V in subfigure of Fig. 5(a). In previous studies, the electrical detection of magnetic resonance demonstrates spin-dependent scattering in the accumulation channel of silicon transistors, which relies on the symmetry of impurity scattering events.[17] Moreover, the weak signals of the four different nuclear spin projections of the arsenic donor were observed in the electrically detected magnetic-resonance measurement.[18] Therefore, the similar fabrication process used in this study implanted arsenic ions in the silicon nanowire. When the external magnetic field polarizes the injection electrons from the source, the polarized electrons transport through the arsenic donor atom of the silicon channel, this process occurs because of magnetic scattering.

According to previous studies, there are two kinds of spin-dependent scattering in two-particle donor states: singlet scattering and triplet scattering. Singlet scattering is a virtual transition to a negatively ionized donor level, where two electrons occupy the same (ground) orbital donor level. Such a transition is symmetrically impossible for triplets, because of Pauli exclusion. Triplet scattering occurs because of virtual transitions into negatively ionized donor levels, where one electron occupies the level and the other electron occupies an excited orbital. These transitions into excited orbital states are also allowed for singlet scattering.[17] Although singlet scattering also has channels for excited orbital states, it is always better for triplet scattering, because the latter has access only to the excited states.[17] Thus, these dI_D/dV_{DS} measurements under magnetic fields suggest a singlet and triplet state of the donor in the transport channel. The two electrons occupy the same orbital donor level, and the donor state is negatively charged (D$^-$); thus, the polarized electrons would not be scattered by the magnetic field. When one electron (D^0) occupies the level, the polarized electrons will be scattered by the parallel spin electron of the same orbital donor level. The schematic diagram of this mechanism is shown in Fig. 5(b).

Because of the difference in singlet and triplet scattering is only single electron transport in the ground state, the weak contribution of the singlet scattering is easily masked in the increasing dI_D/dV_{DS} region (see the $V_G = 0$ and 1 V subfigures of Fig. 5(a)). Thus, singlet and triplet scattering differ slightly and are only observed in the low differential conductance region.

IV. CONCLUSION

We fabricated an n-doped poly-silicon GAA nanowire transistor using standard semiconductor technology and the PADOX method. The Coulomb blockade effect was observed in the silicon nanowire by tunable gate voltage, and fluctuations of the drain current due to Coulomb oscillations and RTS were present, which suggests the two-level trapping state depends on Coulomb oscillations in the transport channel. Under varying magnetic fields, the differential conductance regions of overlapping multiple curves indicate the spin-dependent scattering. This is caused by the spin of arsenic doped, suggesting weak 2-electron singlet-triplet splitting states of the arsenic magnetic impurity. Thus, doping with suitable donors and fabrication of geometric structures provides an effective tool for studying electron motion in quantum physics.

[1]F. A. Zwanenburg, C. van Rijmenam, Y. Fang, C. M. Lieber, and L. P. Kouwenhoven, Nano Lett. **9**, 1071 (2009).
[2]S. C. Rustagi, N. Singh, Y. F. Lim, G. Zhang, S. Wang, G. Q. Lo, N. Balasubramanian, and D. L. Kwong, IEEE Electron Device Lett. **28**, 909 (2007).

[3]Y. S. Sun, Rusli, and N. Singh, IEEE Trans. Nanotechnol. **10**, 96 (2011).

[4]B. H. Hong, L. Choi, Y. C. Jung, S. W. Hwang, K. H. Cho, K. H. Yeo, D. W. Kim, G. Y. Jin, D. Park, S. H. Song, Y. Y. Lee, M. H. Son, and D. Ahn, IEEE Trans. Nanotechnol. **9**, 754 (2010).

[5]J. Zhuge, L. L. Zhang, R. S. Wang, R. Huang, D. W. Kim, D. Park, and Y. Y. Wang, Appl. Phys. Lett. **94**, 083503 (2009).

[6]H. Sellier, G. P. Lansbergen, J. Caro, S. Rogge, N. Collaert, I. Ferain, M. Jurczak, and S. Biesemans, Phys. Rev. Lett. **97**, 206805 (2006).

[7]G. P. Lansbergen, Y. Ono, and A. Fujiwara, Nano Lett. **12**, 763 (2012).

[8]G. P. Lansbergen, R. Rahman, C. J. Wellard, I. Woo, J. Caro, N. Collaert, S. Biesemans, G. Klimeck, L. C. L. Hollenberg, and S. Rogge, Nat. Phys. **4**, 656 (2008).

[9]M. F. Gonzalez-Zalba, D. Heiss, and A. J. Ferguson, New J. Phys. **14**, 023050 (2012).

[10]G. P. Lansbergen, G. C. Tettamanzi, J. Verduijn, N. Collaert, S. Biesemans, M. Blaauboer, and S. Rogge, Nano Lett. **10**, 455 (2010).

[11]Y. Ono, Y. Takahashi, K. Yamazaki, M. Nagase, H. Namatsu, K. Kurihara, and K. Murase, IEEE Trans. Electron Devices **47**, 147 (2000).

[12]M. Nagase, S. Horiguchi, K. Shiraishi, A. Fujiwara, and Y. Takahashi, J. Electroanal. Chem. **559**, 19 (2003).

[13]X. G. Zhang, Z. H. Fang, K. J. Chen, J. Xu, and X. F. Huang, Nanotechnology **22**, 035302 (2011).

[14]*Silicon Nano Electronics*, edited by S. Oda and D. Ferry (Taylor & Francis Group, 2006), pp. 186–187.

[15]E. Prati, M. Belli, M. Fanciulli, and G. Ferrari, Appl. Phys. Lett. **96**, 113109 (2010).

[16]S. Gustavsson, R. Leturcq, B. Simovic, R. Schleser, P. Studerus, T. Ihn, K. Ensslin, D. C. Driscoll, and A. C. Gossard, Phys. Rev. B **74**, 195305 (2006).

[17]R. de Sousa, C. C. Lo, and J. Bokor, Phys. Rev. B **80**, 045320 (2009).

[18]C. C. Lo, V. Lang, R. E. George, J. J. L. Morton, A. M. Tyryshkin, S. A. Lyon, J. Bokor, and T. Schenkel, Phys. Rev. Lett. **106**, 207601 (2011).